Development/Plasticity/Repair

Rapamycin Suppresses Mossy Fiber Sprouting But Not Seizure Frequency in a Mouse Model of Temporal Lobe Epilepsy

Paul S. Buckmaster[1,2] **and Felicia H. Lew**[1,3]

Departments of [1]Comparative Medicine and [2]Neurology and Neurological Sciences, Stanford University, Stanford, California 94305, and [3]College of Veterinary Medicine, Washington State University, Pullman, Washington 99164

Temporal lobe epilepsy is prevalent and can be difficult to treat effectively. Granule cell axon (mossy fiber) sprouting is a common neuropathological finding in patients with mesial temporal lobe epilepsy, but its role in epileptogenesis is unclear and controversial. Focally infused or systemic rapamycin inhibits the mammalian target of rapamycin (mTOR) signaling pathway and suppresses mossy fiber sprouting in rats. We tested whether long-term systemic treatment with rapamycin, beginning 1 d after pilocarpine-induced status epilepticus in mice, would suppress mossy fiber sprouting and affect the development of spontaneous seizures. Mice that had experienced status epilepticus and were treated for 2 months with rapamycin displayed significantly less mossy fiber sprouting (42% of vehicle-treated animals), and the effect was dose dependent. However, behavioral and video/EEG monitoring revealed that rapamycin- and vehicle-treated mice displayed spontaneous seizures at similar frequencies. These findings suggest mossy fiber sprouting is neither pro- nor anti-convulsant; however, there are caveats. Rapamycin treatment also reduced epilepsy-related hypertrophy of the dentate gyrus but did not significantly affect granule cell proliferation, hilar neuron loss, or generation of ectopic granule cells. These findings are consistent with the hypotheses that hilar neuron loss and ectopic granule cells might contribute to temporal lobe epileptogenesis.

Introduction

Granule cell axon (mossy fiber) sprouting is a common neuropathological finding in patients with mesial temporal lobe epilepsy (de Lanerolle et al., 1989; Sutula et al., 1989; Houser et al., 1990) and laboratory animal models (Nadler et al., 1980; Lemos and Cavalheiro, 1995). Normally, granule cells in the dentate gyrus form very few synapses with one another, but sprouted mossy fibers form recurrent, excitatory synapses (Babb et al., 1991; Represa et al., 1993; Franck et al., 1995; Okazaki et al., 1995; Zhang and Houser, 1999; Wenzel et al., 2000b; Buckmaster et al., 2002; Cavazos et al., 2003). Hippocampal slice experiments have shown that after mossy fiber sprouting, granule cells monosynaptically excite one another (Wuarin and Dudek, 1996, 2001; Molnár and Nadler, 1999; Lynch and Sutula, 2000; Scharfman et al., 2003), and seizure-like events are more easily evoked (Patrylo and Dudek, 1998; Gabriel et al., 2004; Winokur et al., 2004). Computer simulations suggest that even modest levels of mossy fiber sprouting substantially promote spread of seizure-like activity (Santhakumar et al., 2005; Dyhrfjeld-Johnsen et al., 2007). Together, these findings support the recurrent excitation hypothesis, which contends that mossy fiber sprouting is epileptogenic (Tauck and Nadler, 1985). In contrast, some have argued that mossy fiber sprouting suppresses seizure activity by activating inhibitory interneurons (Sloviter, 1992; Sloviter et al., 2006).

However, although some *in vivo* studies found correlations between the extent of mossy fiber sprouting and seizure frequency (Mathern et al., 1993, 1997; Lemos and Cavalheiro, 1995; Wenzel et al., 2000b; Pitkänen et al., 2005; Kharatishvili et al., 2006), many have not (Cronin and Dudek, 1988; Masukawa et al., 1992; Mello et al., 1993; Buckmaster and Dudek, 1997; Spencer et al., 1999; Timofeeva and Peterson, 1999; Pitkänen et al., 2000; Wenzel et al., 2000a; Gorter et al., 2001; Nissinen et al., 2001; Zhang et al., 2002; Raol et al., 2003; Jung et al., 2004; Lynd-Balta et al., 2004; Williams et al., 2004; Harvey and Sloviter, 2005; Rao et al., 2006; Kadam and Dudek, 2007). The lack of consistently replicable, statistically significant correlations with *in vivo* seizure activity suggests mossy fiber sprouting might be an epiphenomenon without major pro- or anti-convulsant effects (Gloor, 1997).

Rapamycin might be useful to test the role of mossy fiber sprouting in temporal lobe epileptogenesis. Prolonged, focal infusion of rapamycin into the dentate gyrus inhibits the mammalian target of rapamycin (mTOR) signaling pathway and suppresses mossy fiber sprouting (Buckmaster et al., 2009). Systemic treatment with rapamycin also suppresses mossy fiber sprouting and was reported to reduce seizure frequency in kainate-treated rats (Zeng et al., 2009), which supports the recurrent excitation hypothesis. We sought to further test the recurrent excitation hypothesis and asked the following questions. Does systemic rapamycin suppress mossy fiber sprouting in a mouse model of temporal lobe epilepsy? If so, does it affect the

Received Sept. 15, 2010; revised Nov. 12, 2010; accepted Dec. 10, 2010.

This work was supported by the National Institute of Neurological Disorders and Stroke and National Center for Research Resources. We thank Dr. Xiling Wen for assistance with anatomy.

Correspondence should be addressed to Paul S. Buckmaster, Department of Comparative Medicine, R321 Edwards Building, 300 Pasteur Drive, Stanford University, Stanford, CA 94305. E-mail: psb@stanford.edu.

DOI:10.1523/JNEUROSCI.4852-10.2011

 0270-6474/11/312337-11$15.00/0

frequency or severity of spontaneous seizures? Finally, does rapamycin affect other epilepsy-related abnormalities of dentate gyrus circuitry, including granule cell proliferation, hilar neuron loss, and generation of ectopic granule cells?

Materials and Methods

Animals. All experiments were performed in accordance with the National Institutes of Health *Guide for the Care and Use of Laboratory Animals* and approved by the Stanford University Institutional Animal Care and Use Committee. When they were 48 ± 1 d old, male and female mice of the FVB strain (The Jackson Laboratory) were treated with pilocarpine (300 mg/kg, i.p.) 51 ± 6 min (mean ± SEM) after atropine methylbromide (5 mg/kg, i.p.). Diazepam (10 mg/kg, i.p.) was administered 2 h after the onset of stage 3 or greater seizures (Racine, 1972) and repeated as needed to suppress convulsions. During recovery, mice were kept warm and received lactated Ringer's solution with dextrose. Control mice included animals that were treated identically but did not develop status epilepticus, as well as naive mice.

Rapamycin treatment. Beginning 24 h after pilocarpine treatment, rapamycin was administered systemically using a previously reported dosage regimen that inhibits mTOR activity in the hippocampus (Zeng et al., 2008), except in the present study, treatment was daily instead of 5 d per week. Rapamycin (LC Laboratories) was dissolved initially in 100% ethanol to 20 mg/ml stock solution, which was stored at −20°C. Immediately before injection, stock solution was diluted in 5% Tween 80 and 5% polyethyleneglycol 400 to final concentrations of 4% ethanol and 0.5 or 1 mg/ml rapamycin. Mice were treated daily (intraperitoneally) with 1.5 mg/kg rapamycin, 3 mg/kg rapamycin, or vehicle alone.

Anatomical processing. Mice were killed by urethane overdose (2 g/kg, i.p.) and perfused through the ascending aorta at 15 ml/min for 2 min with 0.9% sodium chloride, 5 min with 0.37% sodium sulfide, 1 min with 0.9% sodium chloride, and 30 min with 4% paraformaldehyde in 0.1 M phosphate buffer (PB; pH 7.4). Brains were postfixed overnight at 4°C. Then, one hippocampus was isolated, cryoprotected in 30% sucrose in PB, gently straightened, frozen, and sectioned transversely with a microtome set at 40 μm. In the present study, the microtome stage was set to advance automatically, which produced sections with an actual thickness very close to 40 μm. In a previous study, the microtome stage was advanced manually, which inadvertently generated thicker sections (Zhang et al., 2009). Subsequently, volume estimates of the present study are more accurate and larger, but relative differences between control and epileptic groups are similar. Volumes of the granule cell layer plus molecular layer of epileptic mice are ~160% of control values in both studies (see below). Sections were collected in 30% ethylene glycol and 25% glycerol in 50 mM PB and stored at −20°C until they were processed together after rinsing in PB.

Starting at a random point near the septal pole, a 1-in-12 series of sections from each hippocampus was mounted, dried, and developed for 45 min in 120 ml of 50% gum arabic, 20 ml of 2 M citrate buffer, 60 ml of 0.5 M hydroquinone, and 1 ml of 19% silver nitrate. After rinsing, sections were exposed to 5% sodium thiosulfate for 4 min before dehydration and coverslipping with DPX. An adjacent 1-in-12 series of sections was processed for Nissl staining with 0.25% thionin. In some cases, a third 1-in-12 series was processed for prox-1 immunoreactivity using a protocol from McCloskey et al. (2006) with slight modifications. Sections were rinsed in PB and treated with 1% H_2O_2 for 2 h. After rinses in PB and 0.1 M Tris-buffered saline (TBS; pH 7.4), sections were treated with blocking solution consisting of 3% goat serum, 2% bovine serum albumin (BSA), and 0.3% Triton X-100 in 0.05 M TBS for 2 h. Sections were rinsed in TBS and incubated for 7 d at 4°C in rabbit anti-prox1 serum (1:40,000, cat. no. PRB-238C, Covance) diluted in 1% goat serum, 0.2% BSA, and 0.3% Triton X-100 in 0.05 M TBS. After rinses in TBS, sections incubated for 2 h in biotinylated goat anti-rabbit serum (1:500; Vector Laboratories) in secondary diluent consisting of 2% BSA and 0.3% Triton X-100 in 0.05 M TBS. After rinses in TBS, sections incubated for 2 h in avidin–biotin–horseradish peroxidase complex (1:500; Vector Laboratories) in secondary diluent. After rinses in TBS and 0.1 M Tris buffer (TB; pH 7.6), sections were placed for 5 min in chromogen solution consisting of 0.02% diaminobenzidine, 0.04% NH_4Cl, and 0.015% glucose oxidase in TB and transferred to fresh chromogen solution with 0.1% β-D-glucose for 13 min. The reaction was stopped in rinses of TB. Sections were mounted and dried on gelatin-coated slides, dehydrated, cleared, and coverslipped with DPX. A similar protocol was used to process tissue from a subset of mice for zinc transporter-3 (ZnT-3) immunoreactivity, except sections incubated for 66 h at 4°C in rabbit anti-ZnT-3 serum (1:5000, catalog # 197002; Synaptic Systems).

Anatomical analyses. Mossy fiber sprouting was measured by estimating the fraction of the entire volume of the granule cell layer plus molecular layer that was black after Timm staining. A 1-in-12 series of sections sampled from the entire septotemporal length of the hippocampus was evaluated (average, 14 sections per mouse). Timm-staining analysis and all other analyses of this study were done by an investigator who was blind as to whether mice had been treated with vehicle versus rapamycin. From each section, an image of the dentate gyrus was obtained with a 10× objective using identical microscope (Axiophot; Zeiss) and camera (Axiocam; Zeiss) settings. NIH ImageJ (1.42q) was used to measure the area of a contour drawn around the granule cell layer plus molecular layer (Fig. 1*D2*). The Timm-positive area within the contour was determined by converting color images to black and white and adjusting a darkness threshold setting until the selected area appeared to match the black Timm-positive area of the same section (Fig. 1*D1*,*D2*). Volumes were calculated by summing areas and multiplying by 12 (section sampling) and 40 μm (section thickness). The percentage of the granule cell layer plus molecular layer that was Timm positive for the entire hippocampus was calculated for each mouse.

Numbers of Nissl-stained granule cells, Nissl-stained hilar neurons, and prox1-immunoreactive hilar neurons per dentate gyrus were estimated using the optical fractionator method and Stereo Investigator (MBF Bioscience). In each case, a 1-in-12 series of sections, randomly and systematically selected from the entire septotemporal length of the hippocampus, was evaluated. A 10× objective was used to draw contours around regions of interest, and a 100× objective was used to count cells. Parameters of stereological analyses are reported in Table 1. For Nissl-stained granule cells, the granule cell layer was analyzed, and granule cell nuclei were counted if they were not cut at the superficial surface of the section. For Nissl-stained hilar neurons, the hilus was outlined along its border with the granule cell layer and straight lines drawn from the ends of the granule cell layer to the proximal end of the CA3 pyramidal cell layer. Nuclei were counted if the maximum diameter of their soma was ≥10 μm and they were not cut at the superficial surface of the section. For prox1-immunopositive hilar neurons, the entire hilar area was sampled, except the region within 25 μm of the granule cell layer, which was excluded. Immunopositive somata were counted if they were not cut at the superficial surface of the section. For each cell type, mean coefficients of error were substantially less than coefficients of variation (Table 1), suggesting sufficient within-animal sampling.

Seizure monitoring. Mice were evaluated for spontaneous seizures by behavioral analysis alone and by video/EEG recording. For behavioral analysis, mice were videotaped 9 h every day. Daily monitoring may be important because, as we observed (data not shown) and others have reported (Goffin et al., 2007; Williams et al., 2009), seizures in individual rodents tend to occur in clusters followed by longer seizure-free periods. Therefore, without daily monitoring for sufficient periods, seizure frequency might be overestimated or underestimated depending on whether monitoring periods coincide with clusters or not. Videotapes were reviewed manually, and motor seizures of stage 3 or greater (Racine, 1972) were counted.

For video/EEG analysis, field potential recordings were obtained from the right, dorsal hippocampus. To implant electrodes, mice were sedated with diazepam (10 mg/kg, i.p.), anesthetized with isoflurane (1–3%), placed in a stereotaxic frame, maintained on a heating pad, and prepared for aseptic surgery. A hole was drilled 1.8 mm posterior and 1.5 mm right of bregma. An insulated, 50-μm-diameter stainless steel wire (California Fine Wire) was implanted 1.7 mm below the surface of the brain. The reference electrode was placed in the cerebellum. The ground was a screw placed rostrally in the skull. Electrode leads were connected to pins that were inserted into a strip connector, which was attached to the skull with

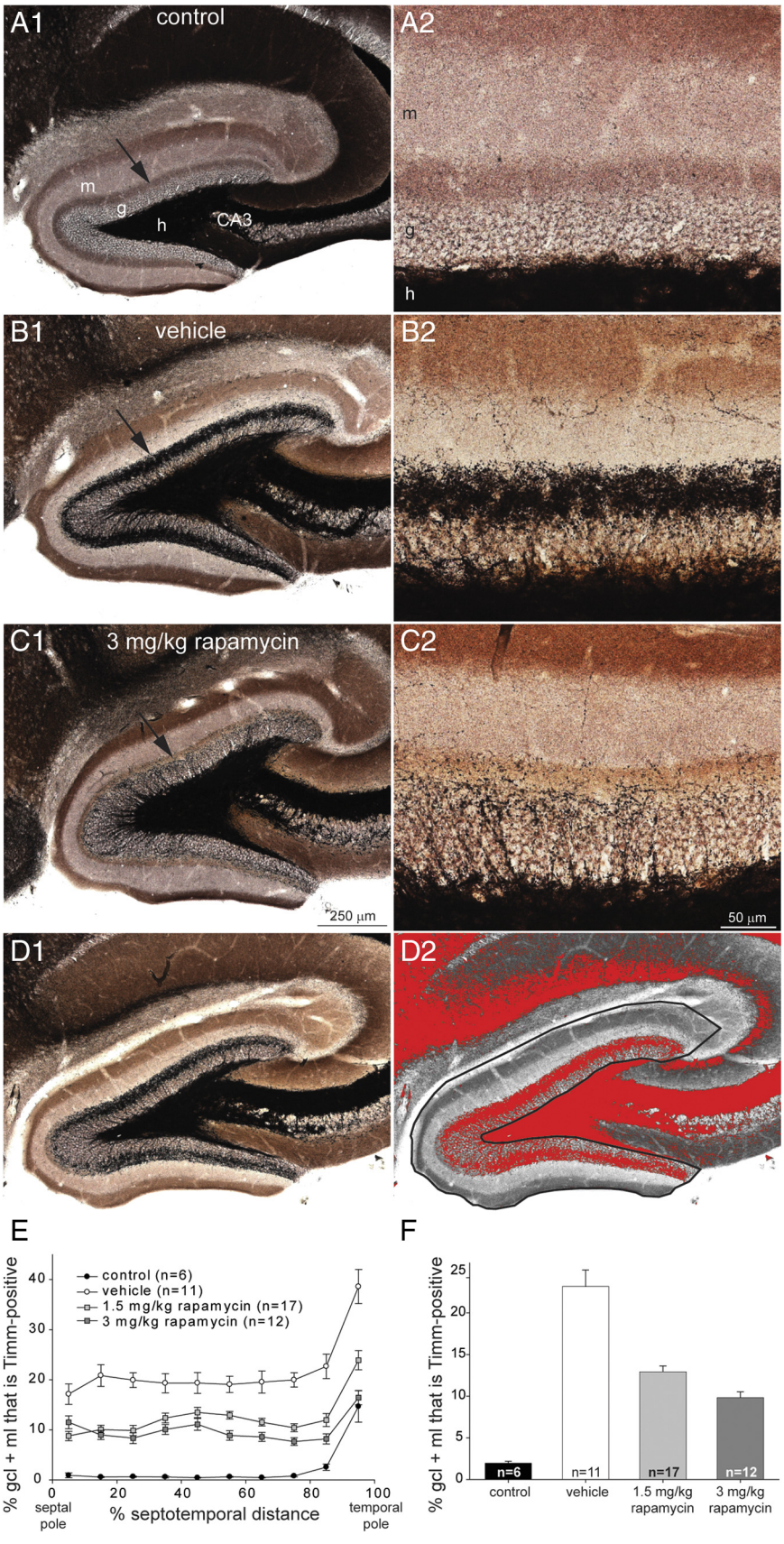

Figure 1. Rapamycin suppresses mossy fiber sprouting in a mouse model of temporal lobe epilepsy. ***A–C***, Timm-stained sections of the dentate gyrus from a control (***A***), a mouse after status epilepticus and treatment for 2 months with vehicle (***B***), and a mouse after status epilepticus and treatment for 2 months with daily, systemic 3 mg/kg rapamycin (***C***). Images on the right (***A2***, ***B2***, ***C2***) are high-magnification views of areas indicated by arrows in the left images. The inner molecular layer is devoid of black Timm staining in the control mouse and displays a prominent band in the vehicle-treated mouse, which is reduced in the rapamycin-treated mouse. m, Molecular layer; g, granule cell layer; h, hilus; CA3, CA3 pyramidal cell layer. ***D***, The method used to quantify mossy fiber sprouting involved making a contour (***D2***, black line) around the granule cell layer plus molecular layer and adjusting a darkness threshold setting until the selected area (***D2***, red) matched the black Timm-positive area of the same section (***D1***). ***E***, Mossy fiber sprouting was suppressed all along the septotemporal axis of the hippocampus by rapamycin treatment. Values represent mean ± SEM. ***F***, Group averages for mossy fiber sprouting in the entire hippocampus. All groups were significantly different from all other groups ($p < 0.05$, ANOVA with Student–Newman–Keuls method). gcl, Granule cell layer; ml, molecular layer.

cranioplastic cement. After surgery, mice were kept warm and received lactated Ringer's solution with dextrose, antibiotic (enrofloxacin, 10 mg/kg, s.c.), and analgesic (buprenorphine, 0.05 mg/kg, s.c.). After recovering for 7 d, mice were monitored 9 h every day by video/EEG recording. Recordings were obtained with AI402 probes and a Cyberamp 380 (Molecular Devices). Signals were amplified 500×, filtered (1–100 Hz), and sampled at 200 Hz (PClamp; Molecular Devices). Electrographic seizures were manually identified as bursts of high-frequency, high-amplitude rhythmic activity that lasted at least 15 s, evolved over time, and exhibited an abrupt onset and offset. All electrographic seizures were evaluated for behavioral correlates, and false-positives attributable to grooming or other artifacts were excluded. Behavioral correlates of electrographically identified seizures were scored according to Racine (1972). Recording electrode locations were verified in Nissl-stained coronal sections.

Unless specified otherwise, chemicals were obtained from Sigma-Aldrich. Statistical analyses were performed using SigmaStat (Systat Software) with $p < 0.05$ considered significant. Values are expressed as mean ± SEM.

Results

Rapamycin suppresses mossy fiber sprouting

In rats, rapamycin suppresses mossy fiber sprouting, even when initiated after an epileptogenic treatment (Buckmaster et al., 2009; Zeng et al., 2009). In control mice, daily 1 mg/kg rapamycin (intraperitoneally) significantly reduces mTOR activity in the hippocampus (Zeng et al., 2008). We tested whether daily 1.5 or 3 mg/kg rapamycin (intraperitoneally) would suppress mossy fiber sprouting in mice that experienced pilocarpine-induced status epilepticus. Rapamycin treatment began 24 h after status epilepticus. Mossy fiber sprouting develops gradually over a period of weeks to months after pilocarpine-induced status epilepticus (Mello et al., 1993). Therefore, daily rapamycin treatment continued for 2 months, at which

Table 1. Parameters of stereological analyses

	Nissl-stained granule cells	Nissl-stained hilar neurons[a]	Prox1-positive hilar neurons
Number of mice	31	48	28
Sections sampled	1 in 12	1 in 12	1 in 12
Counting grid	175 × 175 μm	75 × 75 μm	[b]
Counting frame	10 × 10 μm	50 × 50 μm	[b]
Cells counted/ mouse[c]	149 ± 4	240 ± 21	171 ± 15
Coefficient of variation	0.159	0.368	0.463
Mean coefficient of error[d]	0.075	0.103	0.141

[a]Only somata >10 μm maximum diameter.

[b]Entire hilus evaluated, except the region <25 μm from granule cell layer was excluded.

[c]Mean ± SEM.

[d]Calculated according to West et al. (1991).

time mice were perfused for Timm staining. Mossy fiber sprouting was measured as the fraction of the granule cell layer plus molecular layer that exhibited black Timm staining (Fig. 1*D*). In individual untreated control mice that had not experienced status epilepticus, only 2–4% of the entire granule cell layer plus molecular layer was Timm positive (Fig. 1*A*). The mild level of black Timm staining in control animals is primarily attributable to a projection of mossy fibers into the inner molecular layer at the temporal pole of the hippocampus (Haug, 1974) (Fig. 1*E*). Mice that had experienced status epilepticus and had been treated with vehicle for 2 months displayed a prominent band of black Timm staining in the inner molecular of the dentate gyrus (Fig. 1*B*). Aberrant mossy fiber sprouting in vehicle-treated mice occurred all along the septotemporal axis of the hippocampus (Fig. 1*E*). In individual vehicle-treated mice, 10–34% of the entire granule cell layer plus molecular layer was Timm positive, and the group average (23 ± 2%) was over 10 times greater than that of controls (Fig. 1*F*). Mossy fiber sprouting in rapamycin-treated mice was less than in vehicle-treated animals but more than in controls (Fig. 1*C*,*E*,*F*). In individual mice treated with 1.5 mg/kg rapamycin, 9–19% of the entire granule cell layer plus molecular layer was Timm positive (average, 13 ± 1%). In individual mice treated with 3 mg/kg rapamycin, 7–13% of the granule cell layer plus molecular layer was Timm positive (average, 10 ± 1%), which was less than half (42%) of the amount of mossy fiber sprouting in vehicle-treated mice. All groups were significantly different from each other ($p < 0.05$, ANOVA with Student–Newman–Keuls method) (Fig. 1*F*).

To test the validity of using Timm staining to measure mossy fiber sprouting, adjacent sections from a subset of mice were processed for another marker of mossy fibers. ZnT-3 is expressed most abundantly on synaptic vesicles of granule cell mossy fibers (Wenzel et al., 1997). ZnT-3 immunoreactivity revealed similar patterns of staining as Timm-positive regions of adjacent sections in control mice ($n = 8$) and mice that experienced status epilepticus and were then treated with vehicle ($n = 7$) or 3 mg/kg rapamycin ($n = 7$) (Fig. 2). These findings suggest Timm staining was a reliable label for quantifying extent of mossy fiber sprouting. Together, these findings confirm that even when treatment initiates after an epileptogenic injury, long-term systemic rapamycin suppresses mossy fiber sprouting in rodent models of temporal lobe epilepsy.

Rapamycin does not affect seizure frequency

Systemic rapamycin treatment in a rat model of temporal lobe epilepsy was reported to suppress seizure frequency, even when initiated after status epilepticus (Zeng et al., 2009; Huang et al., 2010). We tested whether daily 3 mg/kg rapamycin (intraperitoneally) would suppress the frequency or severity of spontaneous seizures in mice that experienced pilocarpine-induced status epilepticus. Rapamycin treatment began 24 h after status epilepticus and continued for 2 months. During the second month of treatment, mice were video monitored 9 h every day for spontaneous motor seizures of grade 3 or greater (Racine, 1972). Over 12,600 mouse-hours of data were analyzed, and 2080 motor seizures were identified. Vehicle-treated mice that had experienced status epilepticus ($n = 29$) had 0.02–0.56 seizures per hour. Rapamycin-treated mice that had experienced status epilepticus ($n = 26$) had 0.02–0.32 seizures per hour. Group averages were similar in vehicle- and rapamycin-treated mice (0.168 ± 0.023 and 0.166 ± 0.018 seizures per hour, respectively; $p = 0.7$, *t* test). Seizure severity ranged from forelimb clonus (stage 3), rearing (stage 4), and loss of postural control (stage 5) to wild running (stage 6). Group averages of seizure severity were similar in vehicle- and rapamycin-treated mice (4.64 ± 0.01 and 4.71 ± 0.04, respectively; $p = 0.3$, *t* test). These findings suggest rapamycin does not affect seizure frequency or severity in pilocarpine-treated mice.

To test rapamycin's effect on epileptogenesis more rigorously, we used video/EEG monitoring, evaluated two doses, delayed onset of monitoring for 2 months to allow more time for mossy fiber sprouting to develop, and perfused mice for Timm staining after recording was complete (Fig. 3*A*). Rapamycin treatment began 24 h after status epilepticus, and after almost 2 months, mice were implanted for recording field potentials from the hippocampus ($n = 18$ and 21 for 1.5 and 3 mg/kg rapamycin, respectively). Rapamycin treatment continued while seizure data were collected, because previous findings suggest continued treatment is necessary to keep sprouting suppressed (Buckmaster et al., 2009). When video/EEG recording started during the third month, mice that had been treated with vehicle ($n = 15$) began treatment with 3 mg/kg rapamycin to control for any acute anticonvulsant or pro-convulsant effect that rapamycin might have. Previous findings suggest treating the vehicle group with rapamycin beginning 2 months after status epilepticus is unlikely to reverse already established mossy fiber sprouting (Buckmaster et al., 2009; Zhou et al., 2009). In addition, a group of control mice ($n = 10$) was treated with 3 mg/kg rapamycin and video/EEG monitored to test whether rapamycin was pro-convulsant.

Video/EEG recording lasted up to 1 month, but electrode implants detached early in some cases, and the average duration of recording was 18 d per mouse. Over 10,600 mouse-hours of data were analyzed, and 1480 electrographic seizures were identified. Seizures appeared similar in vehicle- and rapamycin-treated mice and consisted of bursts of high-frequency, high-amplitude rhythmic activity with abrupt onsets and offsets, lasting at least 15 s (Fig. 3*B*). None of the rapamycin-treated control mice that had not experienced status epilepticus displayed seizures. Seizure frequency was similar in vehicle- and rapamycin-treated mice that had experienced status epilepticus ($p > 0.8$, ANOVA) (Fig. 3*F*). Motor seizures of stage 3 or greater (Racine, 1972) accounted for 93% of all electrographic seizures identified. Behavioral seizure severity was similar in vehicle- and 3 mg/kg rapamycin-treated mice (4.60 ± 0.16 and 4.58 ± 0.07, respectively) and slightly more severe in 1.5 mg/kg rapamycin-treated mice (4.93 ± 0.04; $p < 0.05$, ANOVA with Student–Newman–Keuls method).

Timm staining of the dentate gyrus in video/EEG-monitored mice (Fig. 3*C*–*E*) revealed qualitatively similar results to that of mice perfused 2 months after status epilepticus (Fig. 1*A*–*C*). The average percentage of the entire granule cell layer plus molecular layer that was Timm positive was minimal in the control group,

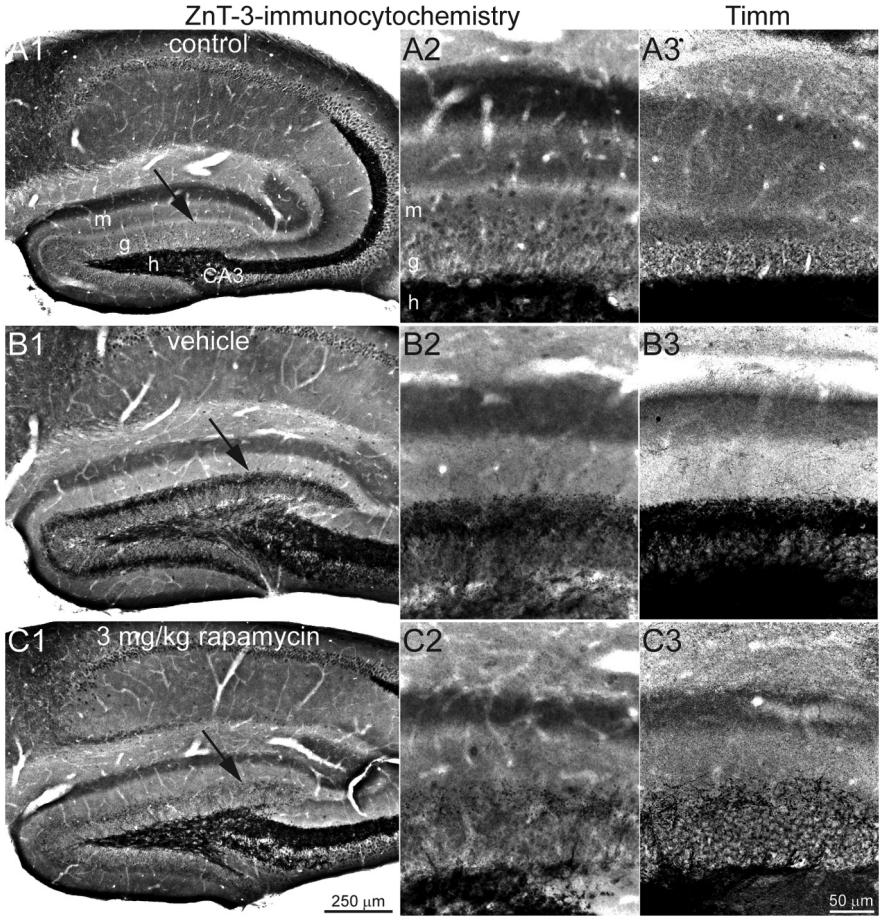

Figure 2. ZnT-3 immunocytochemistry and Timm staining reveal similar patterns of mossy fiber labeling. ZnT-3 immunocytochemistry in the dentate gyrus at low (left) and high (middle) magnification is shown. Arrows in ***A1***, ***B1***, and ***C1*** indicate regions illustrated in ***A2***, ***B2***, and ***C2***. ***A3***, ***B3***, and ***C3*** show a similar region of the dentate gyrus from an adjacent or nearby section in the same hippocampus that was processed for Timm staining. ZnT-3 immunocytochemistry and Timm staining both reveal minimal labeling in the inner molecular layer of the control mouse (***A***), a prominent band of labeling in the mouse that experienced status epilepticus and was treated for 2 months with vehicle (***B***), and reduced labeling in the mouse that experienced status epilepticus and was treated systemically with daily 3 mg/kg rapamycin for 2 months (***C***). m, Molecular layer; g, granule cell layer; h, hilus; CA3, CA3 pyramidal cell layer.

largest in the epileptic vehicle-treated mice, and intermediate in the epileptic rapamycin-treated mice. However, differences between vehicle- and rapamycin-treated groups were smaller after video/EEG recording and 3 months of rapamycin treatment (Fig. 3*G*) than in mice perfused at the 2 month time point (Fig. 1*F*). In video/EEG-monitored 3 mg/kg rapamycin-treated mice, mossy fiber sprouting was reduced to 75% of the level in video/EEG-monitored vehicle-treated animals, whereas, in mice perfused after 2 month treatment with rapamycin, mossy fiber sprouting was reduced to 42% of the level of vehicle-treated animals. To test whether reduced suppression of mossy fiber sprouting might be attributable to surgery for EEG recording versus rapamycin treatment duration or time since status epilepticus, another set of mice ($n = 9$) was treated with daily 3 mg/kg rapamycin for 3 months beginning 1 d after pilocarpine-induced status epilepticus, but they were not implanted for recording field potentials. They displayed a similar level of mossy fiber sprouting (14.9 ± 1.6% of the granule cell layer plus molecular layer) as mice that were treated with 3 mg/kg rapamycin for 3 months and video/EEG recorded (13.7 ± 0.9%; $p = 0.48$, t test). These findings suggest rapamycin's suppressive effect on mossy fiber sprouting decreases during the third month of treatment. During video/EEG monitoring, therefore, the average level of mossy fiber sprouting in mice treated with 3 mg/kg rapamycin probably was reduced to between 42% (at 2 months after status epilepticus, when video/EEG monitoring began) to 75% of that in vehicle-treated epileptic mice (at 3 months after status epilepticus when video/EEG monitoring ceased). In summary, both behavioral and video/EEG seizure monitoring data suggest rapamycin does not affect seizure frequency in pilocarpine-treated mice.

Rapamycin suppresses dentate gyrus hypertrophy

Mouse models of temporal lobe epilepsy display hypertrophy of the dentate gyrus (Bouilleret et al., 1999; Zhang et al., 2009), which might be attributable, at least in part, to mTOR-mediated enlargement of granule cells (Backman et al., 2001; Kwon et al., 2001, 2003, 2006). We evaluated sections from mice described above that had been treated with vehicle or rapamycin for 2 months beginning 24 h after pilocarpine-induced status epilepticus to test whether rapamycin suppresses dentate gyrus hypertrophy. In vehicle-treated mice that had experienced status epilepticus, the average volume of the granule cell layer plus molecular layer in Timm-stained sections was 2.73 ± 0.19 mm^3, which was 158% of controls (1.72 ± 0.07 mm^3; $p < 0.001$, ANOVA with Student–Newman–Keuls method) (Fig. 4*D*). In mice treated with 1.5 mg/kg rapamycin, the average volume of the granule cell layer plus molecular layer was reduced to 2.41 ± 0.06 mm^3 (1.5 mg/kg rapamycin vs control, $p < 0.001$; 1.5 mg/kg rapamycin vs vehicle, $p < 0.03$). In mice treated with 3 mg/kg rapamycin, the average volume of the granule cell layer plus molecular layer was reduced to 2.01 ± 0.07 mm^3 (3 mg/kg rapamycin vs control, $p = 0.12$; 3 mg/kg rapamycin vs vehicle, $p < 0.001$; 3 mg/kg rapamycin vs 1.5 mg/kg rapamycin, $p = 0.007$). These findings suggest rapamycin suppresses dentate gyrus hypertrophy in epileptic pilocarpine-treated mice.

Granule cell somata and dendrites are the major components of the granule cell layer plus molecular layer. Hypertrophy of the region could be attributable to larger granule cells. Another possibility is increased numbers of granule cells, which occurs in epileptic pilocarpine-treated mice (Zhang et al., 2009). We used stereological methods to estimate numbers of granule cells. Control mice had 416,000 ± 13,000 granule cells per hippocampus (Fig. 4*E*). Both vehicle- and 3 mg/kg rapamycin-treated mice that had experienced status epilepticus had more granule cells than controls (141% and 132% of control levels, respectively; $p <$ 0.001, ANOVA with Student–Newman–Keuls method). The difference between vehicle- and rapamycin-treated mice was not statistically significant ($p = 0.15$). These findings are consistent with rapamycin's lack of effect on neurogenesis in kainate-treated rats (Zeng et al., 2009). In addition, these findings suggest rapamycin suppresses epilepsy-related dentate gyrus hypertrophy by

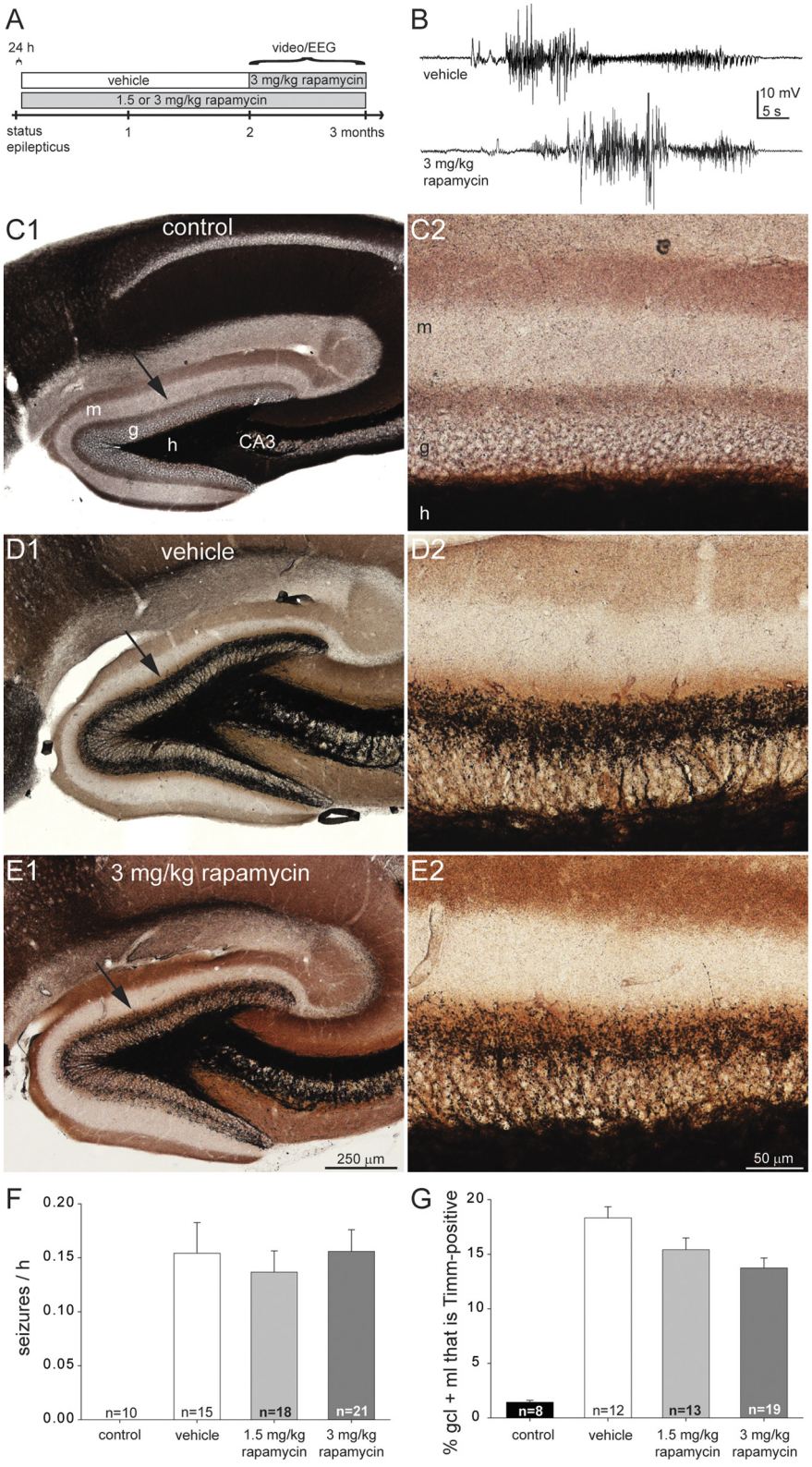

Figure 3. Rapamycin treatment suppresses mossy fiber sprouting but does not affect the frequency of spontaneous seizures in a mouse model of temporal lobe epilepsy. ***A***, Experimental design. ***B***, Spontaneous electrographic seizures recorded in the hippocampus of an epileptic vehicle- and 3 mg/kg rapamycin-treated mouse. ***C–E***, Timm-stained sections of the dentate gyrus from video/EEG-monitored mice: a control (***C***), a mouse after status epilepticus and treatment for 2 months with vehicle (***D***), and a mouse after status epilepticus and treatment for 2 months with daily 3 mg/kg rapamycin (***E***). The inner molecular layer is devoid of black Timm staining in the control mouse and displays a prominent band in the vehicle-treated mouse, which is reduced in the rapamycin-treated mouse. m, Molecular layer; g, granule cell layer; h, hilus; CA3, CA3 pyramidal cell layer. ***F***, Seizure frequency was similar in vehicle- and rapamycin-treated mice that experienced status epilepticus ($p = 0.8$, ANOVA). Rapamycin-treated control mice were never observed to have seizures. Values represent mean ± SEM. ***G***, Mossy fiber sprouting was suppressed by rapamycin. All groups are significantly different from each other ($p < 0.05$, ANOVA with Student–Newman–Keuls method), except there is no significant difference between 1.5 and 3 mg/kg rapamycin-treated mice.

reducing granule cell enlargement, not by inhibiting granule cell proliferation.

Rapamycin does not affect hilar neuron loss

Hilar neuron loss is a common neuropathological feature in patients with temporal lobe epilepsy (Margerison and Corsellis, 1966) and in rodent models (Nadler et al., 1980), including those treated with pilocarpine (Lemos and Cavalheiro, 1995). We used stereological methods to estimate numbers of Nissl-stained hilar neurons with a maximum soma diameter > 10 μm. Control mice ($n = 6$) had 12,500 ± 400 hilar neurons per hippocampus (Fig. 4*F*). Vehicle-treated ($n = 13$), 1.5 mg/kg rapamycin-treated ($n = 14$), and 3 mg/kg rapamycin-treated ($n = 15$) mice that had experienced status epilepticus had fewer hilar neurons (53, 53, and 54% of controls, respectively; $p < 0.001$, ANOVA with Student–Newman–Keuls method). The differences between vehicle- and rapamycin-treated mice were not statistically significant ($p > 0.8$). These findings suggest hilar neuron loss is not affected by rapamycin treatment that begins 24 h after status epilepticus.

Rapamycin does not affect generation of ectopic granule cells

Epileptogenic injuries generate granule cells that become ectopically located in the hilus of rodent models (Houser, 1990; Parent et al., 1997; Jiao and Nadler, 2007) and in patients with temporal lobe epilepsy (Parent et al., 2006). Prox1 is expressed by granule cells (Pleasure et al., 2000; Elliott et al., 2001) including ectopic granule cells but not other hilar neurons (McCloskey et al., 2006). We used stereological methods to estimate numbers of prox1-immunoreactive hilar neurons that were at least 25 μm away from the granule cell layer. Hilar prox1-immunoreactive cells were rare in controls but more common in epileptic vehicle- and rapamycin-treated mice (Fig. 5*A–C*). Control mice ($n = 9$) had 977 ± 71 prox1-positive hilar neurons per hippocampus (Fig. 5*D*). Both vehicle-treated ($n = 9$) and 3 mg/kg rapamycin-treated ($n = 10$) mice that had experienced status epilepticus had over 2.5 times more prox1-positive hilar neu-

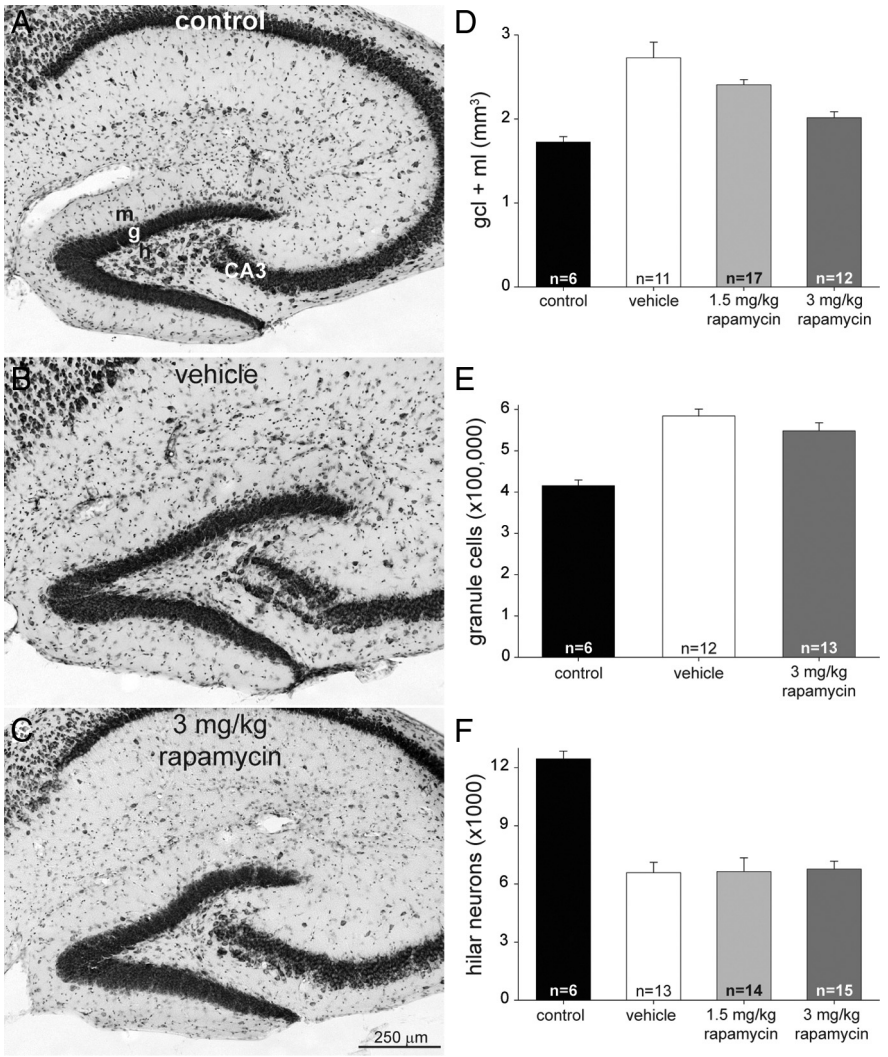

Figure 4. Dentate gyrus volume, granule cell numbers, and hilar neuron numbers in control and epileptic vehicle- and rapamycin-treated mice. ***A–C***, Nissl-stained sections of the dentate gyrus from a control (***A***), a mouse after status epilepticus and treatment for 2 months with vehicle (***B***), and a mouse after status epilepticus and treatment for 2 months with daily 3 mg/kg rapamycin (***C***). m, Molecular layer; g, granule cell layer; h, hilus; CA3, CA3 pyramidal cell layer. ***D***, Epileptic mice display hypertrophy of the granule cell layer (gcl) plus molecular layer (ml), which is suppressed by rapamycin. All groups are significantly different from each other ($p < 0.03$, ANOVA with Student–Newman–Keuls method), except there is no significant difference between control and 3 mg/kg rapamycin-treated groups ($p = 0.12$). Values represent mean ± SEM. ***E***, Vehicle- and rapamycin-treated mice that experience status epilepticus have more granule cells per dentate gyrus than controls ($p < 0.001$, ANOVA with Student–Newman–Keuls method). There is no significant difference between vehicle- and rapamycin-treated groups ($p = 0.15$). ***F***, Numbers of Nissl-stained hilar neurons (with somata >10 μm maximum diameter) per dentate gyrus. Hilar neuron loss is similar in epileptic vehicle- and rapamycin-treated mice ($p > 0.8$, ANOVA with Student–Newman–Keuls method). All groups had significantly fewer hilar neurons than controls ($p < 0.001$).

rons than controls ($p < 0.001$, ANOVA with Student–Newman–Keuls method). The difference between vehicle- and rapamycin-treated mice was not statistically significant ($p = 0.9$). These findings suggest epilepsy-related generation of ectopic granule cells is not affected by rapamycin treatment that begins 1 d after status epilepticus.

Discussion

The principal findings of this study are the following. Systemic treatment with rapamycin beginning 24 h after status epilepticus suppressed mossy fiber sprouting in pilocarpine-treated mice. However, the frequency of spontaneous seizures in rapamycin-treated mice was similar to that of vehicle-treated mice. Treatment with rapamycin diminished epilepsy-related hypertrophy of the dentate gyrus but not granule cell proliferation, hilar neuron loss, or generation of ectopic granule cells. These findings are consistent with hilar neuron loss and ectopic granule cells as epileptogenic mechanisms but raise doubts about the role of mossy fiber sprouting.

Rapamycin suppresses mossy fiber sprouting

Accumulating evidence suggests an important role for the mTOR signaling pathway in mossy fiber sprouting. Treatments that trigger mossy fiber sprouting, including traumatic brain injury (Chen et al., 2007) and status epilepticus (Shacka et al., 2007; Buckmaster et al., 2009; Zeng et al., 2009), activate the mTOR signaling pathway. Activation of the mTOR signaling pathway stimulates axon growth in cultured sensory (Grider et al., 2009) and hippocampal (Choi et al., 2009) neurons. Even without a preceding epileptogenic injury, mossy fiber sprouting develops in transgenic animals with excessive mTOR activity (Kwon et al., 2006), and rapamycin, an inhibitor of mTOR, suppresses axon regeneration (Verma et al., 2005; Park et al., 2008) and guidance of growth cones (Campbell and Holt, 2001).

In the present study, systemic treatment with rapamycin in mice beginning 1 d after pilocarpine-induced status epilepticus significantly reduced mossy fiber sprouting measured 2–3 months later, which is consistent with previous rat studies (Buckmaster et al., 2009; Zeng et al., 2009). Rapamycin appears to be one of the first successful treatments to reduce mossy fiber sprouting when applied after a precipitating injury. Previously, treatment with the protein inhibitor cycloheximide just before an epileptogenic injury was reported to suppress mossy fiber sprouting (Longo and Mello, 1997, 1998; Silva and Mello, 2000). However, cycloheximide protects hilar neurons from excitotoxicity during status epilepticus (Schreiber et al., 1993; Bengzon et al., 1997; Covolan et al., 2000), and extent of mossy fiber sprouting is correlated with the degree of hilar neuron loss (Cavazos and Sutula, 1990; Houser et al., 1990; Babb et al., 1991; Masukawa et al., 1992; Buckmaster and Dudek, 1997; Gorter et al., 2001; Nissinen et al., 2001; Jiao and Nadler, 2007). Therefore, cycloheximide probably reduces mossy fiber indirectly by protecting hilar neurons from excitotoxic damage (Longo et al., 2003). Although rapamycin can protect hilar neurons from excitotoxicity (Zeng et al., 2009), that did not occur in the present study probably because rapamycin treatment was delayed until 1 d after status epilepticus.

Rapamycin is neither anticonvulsant nor antiepileptogenic in the mouse pilocarpine model of temporal lobe epilepsy

Seizure frequency was similar in vehicle- and rapamycin-treated mice, suggesting rapamycin is neither pro-convulsant nor anti-

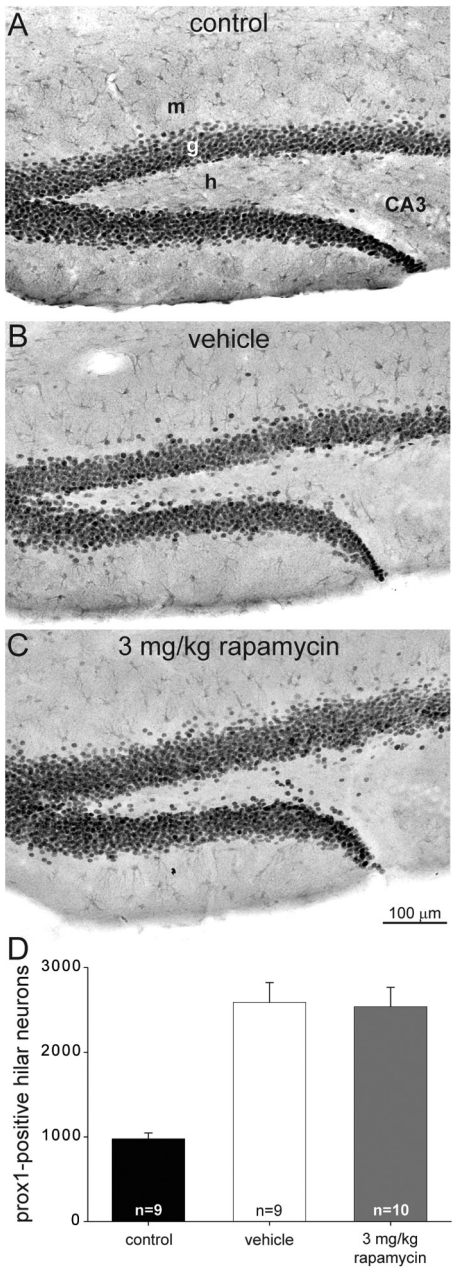

Figure 5. Ectopic granule cells in control and epileptic vehicle- and rapamycin-treated mice. ***A–C***, Prox1-immunostained sections of the dentate gyrus from a control (***A***), a mouse after status epilepticus and treatment for 2 months with vehicle (***B***), and a mouse after status epilepticus and treatment for 2 months with daily 3 mg/kg rapamycin (***C***). m, Molecular layer; g, granule cell layer; h, hilus; CA3, CA3 pyramidal cell layer. ***D***, Numbers of prox1-immunoreactive hilar neurons (≥25 μm away from the granule cell layer) per dentate gyrus. Epileptic vehicle- and rapamycin-treated mice have more prox1-immunopositive hilar neurons than controls ($p < 0.001$, ANOVA with Student–Newman–Keuls method). There is no significant difference between the vehicle- and rapamycin-treated groups ($p = 0.9$). Values represent mean ± SEM.

convulsant. Previous reports on rapamycin's effects on seizure activity are mixed. Rapamycin does not alter evoked field potentials in CA1 of hippocampal slices from rats (Daoud et al., 2007) and has either no effect or inhibits spontaneous action potential firing in hippocampal neuron cultures from rats (Rüegg et al., 2007). Rapamycin was reported to be anticonvulsant when administered to pilocarpine-treated rats after they had developed chronic, spontaneous, recurrent seizures (Huang et al., 2010). However, severity of chemically induced status epilepticus is similar in rats with and without prior rapamycin treatment (Zeng et al., 2009; Huang et al., 2010).

In rodent models of conditions such as tuberous sclerosis that involve mutations causing excessive activity of the mTOR signaling pathway, seizures are common (Backman et al., 2001; Kwon et al., 2001, 2006; Uhlmann et al., 2002; Meikle et al., 2007), and rapamycin (Zeng et al., 2008; Ljungberg et al., 2009; Zhou et al., 2009) and other inhibitors of mTOR (Kwon et al., 2003) reduce seizure frequency. In rodent models of temporal lobe epilepsy, rapamycin's effects are less clear. In contrast to pilocarpine-treated mice in the present study, rapamycin reduced seizure frequency in kainate-treated rats (Zeng et al., 2009). Possible explanations for the apparently contradictory results include differences in the timing and methods of seizure monitoring or a confounding anticonvulsant effect of rapamycin specifically in rats (Huang et al., 2010).

Is mossy fiber sprouting epileptogenic?

Rapamycin significantly reduced mossy fiber sprouting without affecting the frequency of spontaneous seizures in pilocarpine-treated mice. This finding suggests that mossy fiber sprouting might be an epiphenomenon without major antiepileptogenic or pro-epileptogenic effects; however, there are caveats. Ideally, to evaluate its role in epileptogenesis, mossy fiber sprouting would be blocked completely. In the present study, mossy fiber sprouting was reduced to 42–75% of levels found in vehicle-treated epileptic mice. There may be a threshold effect such that beyond a critical level, mossy fiber sprouting dramatically increases the probability of seizures. Computer simulations suggest relatively small amounts of mossy fiber sprouting might be sufficient to increase seizure susceptibility (Santhakumar et al., 2005; Dyhrfjeld-Johnsen et al., 2007). However, it is unlikely that higher doses of rapamycin would completely block mossy fiber sprouting. Focal infusion of up to 10 mM rapamycin directly into the dentate gyrus did not entirely block mossy fiber sprouting (Buckmaster et al., 2009). The 3 mg/kg dose used in the present study virtually eliminated hippocampal mTOR activity in control mice of a previous study (Zeng et al., 2008) and reduced dentate gyrus hypertrophy to levels not significantly different from non-epileptic controls. Signaling pathways that control processes such as axon growth, pathfinding, and synaptogenesis are likely to be redundant and resistant to complete suppression by inhibiting a single important node (Bromberg et al., 2008).

Another caveat is that epileptogenesis might have been maintained by rapamycin-related side effects or other "compensatory" changes. For example, GABAergic interneuron axons in the dentate gyrus sprout and form more synapses with granule cells after epileptogenic injuries (Babb et al., 1989; Zhang et al., 2009; Thind et al., 2010). If rapamycin also suppresses GABAergic axon sprouting, it might counteract the effect of reduced mossy fiber sprouting. In addition, other recurrent excitatory circuits with granule cells might compete with sprouted mossy fibers for synaptic targets on granule cell dendrites. If competing axons were resistant to rapamycin, they might develop excessively when mossy fiber sprouting is reduced. Possibilities include axon sprouting by surviving mossy cells (Namgung et al., 1997; Del Turco et al., 2003; Prang et al., 2003) and CA3 pyramidal cells (Bausch and McNamara, 2004; Siddiqui and Joseph, 2005; Rao et al., 2006).

Finally, the lack of effect of reduced mossy fiber sprouting on epileptogenesis might be attributable to limitations of the model. Status epilepticus-based rodent models replicate many neuro-

pathological features found in patients with temporal lobe epilepsy, including mossy fiber sprouting. However, there are potentially important differences. For example, excitotoxic damage appears to involve extrahippocampal structures to a greater degree in rodent models compared with patients (Chen and Buckmaster, 2005). Some have argued that chemoconvulsant rodent models are invalid for this experimental question, because their seizures might initiate by different mechanisms and in different brain regions than in patients with temporal lobe epilepsy (Mello et al., 1996; Harvey and Sloviter, 2005; Sloviter et al., 2006). However, fos labeling reveals early activation of granule cells during spontaneous seizures in epileptic pilocarpine-treated mice (Peng and Houser, 2005), suggesting they are a reasonable model in which to test the role of mossy fiber sprouting.

Other potentially epileptogenic changes

Some epilepsy-related abnormalities observed in the present study are unlikely to contribute to temporal lobe epileptogenesis (e.g., granule cell hypertrophy). Transgenic mice with excessive activation of the mTOR signaling pathway display enlarged granule cell somata (Backman et al., 2001; Kwon et al., 2001, 2003; Way et al., 2009) and dendrites (Kwon et al., 2006), which can be reversed by rapamycin (Zhou et al., 2009). In the present study, rapamycin reduced hypertrophy nearly to control levels without affecting seizure frequency. An epilepsy-related net increase in granule cell numbers seems unlikely to be epileptogenic, because it does not occur in epileptic pilocarpine-treated rats (Thind et al., 2010) or patients with temporal lobe epilepsy (Mouritzen Dam, 1980; Mathern et al., 1995).

On the other hand, results of the present study are consistent with other potential epileptogenic mechanisms. Almost half the hilar neuron population was killed presumably by status epilepticus in vehicle- and rapamycin-treated mice. In control animals, ~60% of hilar neurons are excitatory mossy cells, and ~40% are inhibitory GABAergic interneurons (Buckmaster and Jongen-Rêlo, 1999; Jiao and Nadler, 2007). Loss of mossy cells (Sloviter et al., 2003) and interneurons (de Lanerolle et al., 1989) has been proposed as epileptogenic mechanisms. Ectopic granule cells receive aberrant excitatory synaptic input from other granule cells (Dashtipour et al., 2001; Pierce et al., 2005). They display abnormal circuitry (Scharfman et al., 2000) and abnormal intrinsic electrophysiological properties (Zhan and Nadler, 2009). Their numbers correlate with seizure frequency in epileptic pilocarpine-treated rats (McCloskey et al., 2006), and reducing the generation of ectopic granule cells was reported to suppress epileptogenesis (Jung et al., 2004). Results of the present study are consistent with an epileptogenic role for ectopic granule cells. In summary, rapamycin's effects are complicated but helpful for prioritizing epilepsy-related changes that might affect seizure generation.

References

Babb TL, Pretorius JK, Kupfer WR, Crandall PH (1989) Glutamate decarboxylase-immunoreactive neurons are preserved in human epileptic hippocampus. J Neurosci 9:2562–2574.

Babb TL, Kupfer WR, Pretorius JK, Crandall PH, Levesque MF (1991) Synaptic reorganization by mossy fibers in human epileptic fascia dentata. Neuroscience 42:351–363.

Backman SA, Stambolic V, Suzuki A, Haight J, Elia A, Pretorius J, Tsao M-S, Shannon P, Bolon B, Ivy GO, Mak TW (2001) Deletion of Pten in mouse brain causes seizures ataxia and defects in soma size resembling Lhermitte-Duclos disease. Nat Genet 29:396–403.

Bausch SB, McNamara JO (2004) Contributions of mossy fiber and CA1 pyramidal cell sprouting to dentate granule cell hyperexcitability in kainic acid-treated hippocampal slice cultures. J Neurophysiol 92:3582–3595.

Bengzon J, Kokaia Z, Elmér E, Nanobashvili A, Kokaia M, Lindvall O (1997) Apoptosis and proliferation of dentate gyrus neurons after single and intermittent limbic seizures. Proc Natl Acad Sci U S A 94:10432–10437.

Bouilleret V, Ridoux V, Depaulis A, Marescaux C, Nehlig A, Le Gal La Salle G (1999) Recurrent seizures and hippocampal sclerosis following intrahippocampal kainate injection in adult mice: electroencephalography, histopathology and synaptic reorganization similar to mesial temporal lobe epilepsy. Neuroscience 89:717–729.

Bromberg KD, Ma'ayan A, Neves SR, Iyengar R (2008) Design logic of a cannabinoid receptor signaling network that triggers neurite outgrowth. Science 320:903–909.

Buckmaster PS, Dudek FE (1997) Neuron loss, granule cell axon reorganization, and functional changes in the dentate gyrus of epileptic kainate-treated rats. J Comp Neurol 385:385–404.

Buckmaster PS, Jongen-Rêlo AL (1999) Highly specific neuron loss preserves lateral inhibitory circuits in the dentate gyrus of kainate-induced epileptic rats. J Neurosci 19:9519–9529.

Buckmaster PS, Zhang GF, Yamawaki R (2002) Axon sprouting in a model of temporal lobe epilepsy creates a predominantly excitatory feedback circuit. J Neurosci 22:6650–6658.

Buckmaster PS, Ingram EA, Wen X (2009) Inhibition of the mammalian target of rapamycin signaling pathway suppresses dentate granule cell axon sprouting in a rodent model of temporal lobe epilepsy. J Neurosci 29:8259–8269.

Campbell DS, Holt CE (2001) Chemotropic responses of retinal growth cones mediated by rapid local protein synthesis and degradation. Neuron 32:1013–1026.

Cavazos JE, Sutula TP (1990) Progressive neuronal loss induced by kindling: a possible mechanism for mossy fiber synaptic reorganization and hippocampal sclerosis. Brain Res 527:1–6.

Cavazos JE, Zhang P, Qazi R, Sutula TP (2003) Ultrastructural features of sprouted mossy fiber synapses in kindled and kainic acid-treated rats. J Comp Neurol 458:272–292.

Chen S, Buckmaster PS (2005) Stereological analysis of forebrain regions in kainate-treated epileptic rats. Brain Res 1057:141–152.

Chen S, Atkins CM, Liu CL, Alonso OF, Dietrich WD, Hu BR (2007) Alterations in mammalian target of rapamycin signaling pathways after traumatic brain injury. J Cereb Blood Flow Metab 27:939–949.

Choi Y-J, Di Nardo A, Kramvis I, Meikle L, Kwiatkowski DJ, Sahin M, He X (2009) Tuberous sclerosis complex proteins control axon formation. Gen Dev 22:2485–2495.

Covolan L, Ribeiro LTC, Longo BM, Mello LEAM (2000) Cell damage and neurogenesis in the dentate granule cell layer of adult rats after pilocarpine- or kainate-induced status epilepticus. Hippocampus 10:169–180.

Cronin J, Dudek FE (1988) Chronic seizures and collateral sprouting of dentate mossy fibers after kainic acid treatment in rats. Brain Res 474:181–184.

Daoud D, Scheld HH, Speckmann E-J, Gorji A (2007) Rapamycin: brain excitability studied in vitro. Epilepsia 48:834–836.

Dashtipour K, Tran PH, Okazaki MM, Nadler JV, Ribak CE (2001) Ultrastructural features and synaptic connections of hilar ectopic granule cells in the rat dentate gyrus are different from those of granule cells in the granule cell layer. Brain Res 890:261–271.

de Lanerolle NC, Kim JH, Robbins RJ, Spencer DD (1989) Hippocampal interneuron loss and plasticity in human temporal lobe epilepsy. Brain Res 495:387–395.

Del Turco D, Woods AG, Gebhardt C, Phinney AL, Jucker M, Frotscher M, Deller T (2003) Comparison of commissural sprouting in the mouse rat fascia dentata after entorhinal cortex lesion. Hippocampus 13:685–699.

Dyhrfjeld-Johnsen J, Santhakumar V, Morgan RJ, Huerta R, Tsimring L, Soltesz I (2007) Topological determinants of epileptogenesis in large-scale structural and functional models of the dentate gyrus derived from experimental data. J Neurophysiol 97:1566–1587.

Elliott RC, Khademi S, Pleasure SJ, Parent JM, Lowenstein DH (2001) Differential regulation of basic helix-loop-helix mRNAs in the dentate gyrus following status epilepticus. Neuroscience 106:79–88.

Franck JE, Pokorny J, Kunkel DD, Schwartzkroin PA (1995) Physiologic and morphologic characteristics of granule cell circuitry in human epileptic hippocampus. Epilepsia 36:543–558.

Gabriel S, Njunting M, Pomper JK, Merschhemke M, Sanabria ERG, Eilers A, Kivi A, Zeller M, Meencke H-J, Cavalheiro EA, Heinemann U, Lehmann T-N (2004) Stimulus and potassium-induced epileptiform activity in

the human dentate gyrus from patients with and without hippocampal sclerosis. J Neurosci 24:10416–10430.
Gloor P (1997) The temporal lobe and limbic system, pp 677–691. New York: Oxford UP.
Goffin K, Nissinen J, Van Laere K, Pitkänen A (2007) Cyclicity of spontaneous recurrent seizures in pilocarpine model of temporal lobe epilepsy in rat. Exp Neurol 205:501–505.
Gorter JA, van Vliet EA, Aronica E, Lopes da Silva FH (2001) Progression of spontaneous seizures after status epilepticus is associated with mossy fibre sprouting and extensive bilateral loss of hilar parvalbumin and somatostatin-immunoreactive neurons. Eur J Neurosci 13:657–669.
Grider MH, Park D, Spencer DM, Shine HD (2009) Lipid raft-targeted Akt promotes axonal branching and growth cone expansion via mTOR and Rac1, respectively. J Neurosci Res 87:3033–3042.
Harvey BD, Sloviter RS (2005) Hippocampal granule cell activity and c-fos expression during spontaneous seizures in awake, chronically epileptic, pilocarpine-treated rats: implications for hippocampal epileptogenesis. J Comp Neurol 488:442–463.
Haug, F-M Š (1974) Light microscopical mapping of the hippocampal region, the piriform cortex and the corticomedial amygdaloid nuclei of the rat with Timm's sulphide silver method. Z Anat Entwickl-Gesch 145:1–27.
Houser CR (1990) Granule cell dispersion in the dentate gyrus of humans with temporal lobe epilepsy. Brain Res 535:195–204.
Houser CR, Miyashiro JE, Swartz BE, Walsh GO, Rich JR, Delgado-Escueta AV (1990) Altered patterns of dynorphin immunoreactivity suggest mossy fiber reorganization in human hippocampal epilepsy. J Neurosci 10:267–282.
Huang X, Zhang H, Yang J, Wu J, McMahon J, Lin Y, Cao Z, Gruenthal M, Huang Y (2010) Pharmacological inhibition of the mammalian target of rapamycin pathway suppresses acquired epilepsy. Neurobiol Dis 40:193–199.
Jiao Y, Nadler JV (2007) Stereological analysis of GluR2-immunoreactive hilar neurons in the pilocarpine model of temporal lobe epilepsy: correlation of cell loss with mossy fiber sprouting. Exp Neurol 205:569–582.
Jung K-H, Chu K, Kim M, Jeong S-W, Song Y-M, Lee S-T, Kim J-Y, Lee SK, Roh J-K (2004) Continuous cytosine-b-D-arabinofuranoside infusion reduces ectopic granule cells in adult rat hippocampus with attenuation of spontaneous recurrent seizures following pilocarpine-induced status epilepticus. Eur J Neurosci 19:3219–3226.
Kadam SD, Dudek FE (2007) Neuropathological features of a rat model for perinatal hypoxic-ischemic encephalopathy with associated epilepsy. J Comp Neurol 505:716–737.
Kharatishvili I, Nissinen JP, McIntosh TK, Pitkänen A (2006) A model of posttraumatic epilepsy induced by lateral fluid-percussion brain injury in rats. Neuroscience 140:685–697.
Kwon C-H, Zhu X, Zhang J, Knoop LL, Tharp R, Smeyne RJ, Eberhart CG, Burger PC, Baker SJ (2001) Pten regulates neuronal soma size: a mouse model of Lhermitte-Duclos disease. Nat Gen 29:404–411.
Kwon C-H, Zhu X, Zhang J, Baker SJ (2003) mTor is required for hypertrophy of Pten-deficient neuronal soma in vivo. Proc Natl Acad Sci U S A 100:12923–12928.
Kwon C-H, Luikart BW, Powell CM, Zhou J, Matheny SA, Zhang W, Li Y, Baker SJ, Parada LF (2006) Pten regulates neuronal arborization and social interaction in mice. Neuron 50:377–388.
Lemos T, Cavalheiro EA (1995) Suppression of pilocarpine-induced status epilepticus and the late development of epilepsy in rats. Exp Brain Res 102:423–428.
Ljungberg MC, Sunnen CN, Lugo JN, Anderson AE, D'Arcangelo G (2009) Rapamycin suppresses seizures and neuronal hypertrophy in a mouse model of cortical dysplasia. Dis Model Mech 2:389–398.
Longo BM, Mello LEAM (1997) Blockade of pilocarpine- or kainate-induced mossy fiber sprouting by cycloheximide does not prevent subsequent epileptogenesis in rats. Neurosci Lett 226:163–166.
Longo BM, Mello LEAM (1998) Supragranular mossy fiber sprouting is not necessary for spontaneous seizures in the intrahippocampal kainate model of epilepsy in the rat. Epilepsy Res 32:172–182.
Longo BM, Covolan L, Chadi G, Mello LEAM (2003) Sprouting of mossy fibers and the vacating of postsynaptic targets in the inner molecular layer of the dentate gyrus. Exp Neurol 181:57–67.
Lynch M, Sutula T (2000) Recurrent excitatory connectivity in the dentate gyrus of kindled and kainic acid-treated rats. J Neurophysiol 83:693–704.
Lynd-Balta E, Pilcher WH, Joseph SA (2004) AMPA receptor alterations precede mossy fiber sprouting in young children with temporal lobe epilepsy. Neuroscience 126:105–114.
Margerison JH, Corsellis JAN (1966) Epilepsy and the temporal lobes. Brain 89:499–530.
Masukawa LM, Uruno K, Sperling M, O'Connor MJ, Burdette LJ (1992) The functional relationship between antidromically evoked field responses of the dentate gyrus and mossy fiber reorganization in temporal lobe epileptic patients. Brain Res 579:119–127.
Mathern GW, Cifuentes F, Leite JP, Pretorius JK, Babb TL (1993) Hippocampal EEG excitability and chronic spontaneous seizures are associated with aberrant synaptic reorganization in the rat intrahippocampal kainate model. EEG Clin Neurophysiol 87:326–339.
Mathern GW, Pretorius JK, Babb TL (1995) Quantified patterns of mossy fiber sprouting and neuron densities in hippocampal and lesional seizures. J Neurosurg 82:211–219.
Mathern GW, Bertram EH III, Babb TL, Pretorius JK, Kuhlman PA, Spradlin S, Mendoza D (1997) In contrast to kindled seizures, the frequency of spontaneous epilepsy in the limbic status model correlates with greater aberrant fascia dentate excitatory and inhibitory axon sprouting, and increased staining for N-methyl-D-aspartate, AMPA and $GABA_A$ receptors. Neuroscience 77:1003–1019.
McCloskey DP, Hintz TM, Pierce JP, Scharfman HE (2006) Stereological methods reveal the robust size and stability of ectopic hilar granule cells after pilocarpine-induced status epilepticus in the adult rat. Eur J Neurosci 24:2203–2210.
Meikle L, Talos DM, Onda H, Pollizzi K, Rotenberg A, Sahin M, Jensen FE, Kwiatkowski DJ (2007) A mouse model of tuberous sclerosis: neuronal loss of Tsc1 causes dysplastic and ectopic neurons, reduced myelination, seizure activity, and limited survival. J Neurosci 27:5546–5558.
Mello LEAM, Cavalheiro EA, Tan AM, Kupfer WR, Pretorius JK, Babb TL, Finch DM (1993) Circuit mechanisms of seizures in the pilocarpine model of chronic epilepsy: cell loss and mossy fiber sprouting. Epilepsia 34:985–995.
Mello LEAM, Kohman CM, Tan AM, Cavalheiro EA, Finch DM (1996) Lack of Fos-like immunoreactivity after spontaneous seizures or reinduction of status epilepticus by pilocarpine in rats. Neurosci Lett 208:133–137.
Molnár P, Nadler JV (1999) Mossy fiber–granule cell synapses in the normal and epileptic rat dentate gyrus studied with minimal laser photostimulation. J Neurophysiol 82:1883–1894.
Mouritzen Dam A (1980) Epilepsy and neuron loss in the hippocampus. Epilepsia 21:617–629.
Nadler JV, Perry BW, Cotman CW (1980) Selective reinnervation of hippocampal area CA1 and the fascia dentata after destruction of CA3-CA4 afferents with kainic acid. Brain Res 182:1–9.
Namgung U, Matsuyama S, Routtenberg A (1997) Long-term potentiation activates the GAP-43 promotor: selective participation of hippocampal mossy cells. Proc Natl Acad Sci U S A 94:11675–11680.
Nissinen J, Lukasiuk K, Pitkänen A (2001) Is mossy fiber sprouting present at the time of the first spontaneous seizures in rat experimental temporal lobe epilepsy? Hippocampus 11:299–310.
Okazaki MM, Evenson DA, Nadler JV (1995) Hippocampal mossy fiber sprouting and synapse formation after status epilepticus in rats: visualization after retrograde transport of biocytin. J Comp Neurol 352:515–534.
Parent JM, Yu TW, Leibowitz RT, Geschwind DH, Sloviter RS, Lowenstein DH (1997) Dentate granule cell neurogenesis is increased by seizures and contributes to aberrant network reorganization in the adult rat hippocampus. J Neurosci 17:3727–3738.
Parent JM, Pleasure SJ, Barbaro NM, Lowenstein DH (2006) Aberrant seizure-induced neurogenesis in experimental temporal lobe epilepsy. Ann Neurol 59:81–91.
Park KK, Liu K, Hu Y, Smith PD, Wang C, Cai B, Xu B, Connolly L, Kramvis I, Sahin M, He Z (2008) Promoting axon regeneration in the adult CNS by modulation of the PTEN/mTOR pathway. Science 322:963–966.
Patrylo PR, Dudek FE (1998) Physiological unmasking of new glutamatergic pathways in the dentate gyrus of hippocampal slices form kainate-induced epileptic rats. J Neurophysiol 79:418–429.
Peng Z, Houser CR (2005) Temporal patterns of fos expression in the dentate gyrus after spontaneous seizures in a mouse model of temporal lobe epilepsy. J Neurosci 25:7210–7220.
Pierce JP, Melton J, Punsoni M, McCloskey DP, Scharfman HE (2005)

Mossy fibers are the primary source of afferent input to ectopic granule cells that are born after pilocarpine-induced seizures. Exp Neurol 196:316–331.

Pitkänen A, Nissinen J, Lukasiuk K, Jutila L, Paljärvi L, Salmenperä T, Karkola K, Vapalahti M, Ylinen A (2000) Association between the density of mossy fiber sprouting and seizure frequency in experimental and human temporal lobe epilepsy. Epilepsia 41 [Suppl 6]:S24–S29.

Pitkänen A, Kharatishvili I, Narkilahti S, Lukasiuk K, Nissinen J (2005) Administration of diazepam during status epilepticus reduces development and severity of epilepsy in rat. Epilepsy Res 63:27–42.

Pleasure SJ, Collins AE, Lowenstein DH (2000) Unique expression patterns of cell fate molecules delineate sequential stages of dentate gyrus development. J Neurosci 20:6095–6105.

Prang P, Del Turco D, Deller T (2003) Associational sprouting in the mouse fascia dentata after entorhinal lesion in vitro. Brain Res 978:205–212.

Racine RJ (1972) Modification of seizure activity by electrical stimulation: II. Motor seizure. Electroencephalogr Clin Neurophysiol 32:281–294.

Rao MS, Hattiangady B, Reddy DS, Shetty AK (2006) Hippocampal neurodegeneration, spontaneous seizures, and mossy fiber sprouting in the F344 rat model of temporal lobe epilepsy. J Neurosci Res 83:1088–1105.

Raol VSH, Budreck EC, Brooks-Kayal AR (2003) Epilepsy after early-life seizures can be independent of hippocampal injury. Ann Neurol 53:503–511.

Represa A, Jorquera I, Le Gal La Salle G, Ben-Ari Y (1993) Epilepsy induced collateral sprouting of hippocampal mossy fibers: does it induce the development of ectopic synapses with granule cell dendrites? Hippocampus 3:257–268.

Rüegg S, Baybis M, Juul H, Dichter M, Crino PB (2007) Effects of rapamycin on gene expression, morphology, and electrophysiological properties of rat hippocampal neurons. Epilepsy Res 77:85–92.

Santhakumar V, Aradi I, Soltesz I (2005) Role of mossy fiber sprouting and mossy cell loss in hyperexcitability: a network model of the dentate gyrus incorporating cell types and axonal topography. J Neurophysiol 93:437–453.

Scharfman HE, Goodman JH, Sollas AL (2000) Granule-like neurons at the hilar/CA3 border after status epilepticus and their synchrony with area CA3 pyramidal cells: functional implications of seizure-induced neurogenesis. J Neurosci 20:6144–6158.

Scharfman HE, Sollas AL, Berger RE, Goodman JH (2003) Electrophysiological evidence of monosynaptic excitatory transmission between granule cells after seizure-induced mossy fiber sprouting. J Neurophysiol 90:2536–2547.

Schreiber SS, Tocco G, Najm I, Thompson RF, Baudry M (1993) Cycloheximide prevents kainate-induced neuronal death and c-fos expression in adult rat brain. J Mol Neurosci 4:149–159.

Shacka JJ, Lu J, Xie Z-L, Uchiyama Y, Roth KA, Zhang J (2007) Kainic acid induces early and transient autophagic stress in mouse hippocampus. Neurosci Lett 414:57–60.

Siddiqui AH, Joseph SA (2005) CA3 axonal sprouting in kainate-induced chronic epilepsy. Brain Res 1066:129–146.

Silva JG, Mello LEAM (2000) The role of mossy cell death and activation of protein synthesis in the sprouting of dentate mossy fibers: evidence from calretinin and neo-Timm staining in pilocarpine-epileptic mice. Epilepsia 41 [Suppl 6]:S18–S23.

Sloviter RS (1992) Possible functional consequences of synaptic reorganization in the dentate gyrus of kainate-treated rats. Neurosci Lett 137:91–96.

Sloviter RS, Zappone CA, Harvey BD, Bumanglag AV, Bender RA, Frotscher M (2003) "Dormant basket cell" hypothesis revisited: relative vulnerabilities of dentate gyrus mossy cells and inhibitory interneurons after hippocampal status epilepticus in the rat. J Comp Neurol 459:44–76.

Sloviter RS, Zappone CA, Harvey BD, Frotscher M (2006) Kainic acid-induced recurrent mossy fiber innervation of dentate gyrus inhibitory interneurons: possible anatomical substrate of granule cell hyperinhibition in chronically epileptic rats. J Comp Neurol 494:944–960.

Spencer SS, Kim J, de Lanerolle N, Spencer DD (1999) Differential neuronal and glial relations with parameters of ictal discharge in mesial temporal lobe epilepsy. Epilepsia 40:708–712.

Sutula T, Cascino G, Cavazos J, Parada I, Ramirez L (1989) Mossy fiber synaptic reorganization in the epileptic human temporal lobe. Ann Neurol 26:321–330.

Tauck DL, Nadler JV (1985) Evidence of functional mossy fiber sprouting in hippocampal formation of kainic acid-treated rats. J Neurosci 5:1016–1022.

Thind KK, Yamawaki R, Phanwar I, Zhang G, Wen X, Buckmaster PS (2010) Initial loss but later excess of GABAergic synapses with dentate granule cells in a rat model of temporal lobe epilepsy. J Comp Neurol 518:647–667.

Timofeeva OA, Peterson GM (1999) Dissociation of mossy fiber sprouting and electrically-induced seizure sensitivity: rapid kindling versus adaptation. Epilepsy Res 33:99–115.

Uhlmann EJ, Wong M, Baldwin RL, Bajenaru ML, Onda H, Kwiatkowski DJ, Yamada K, Gutman DH (2002) Astroctye-specific TSC1 conditional knockout mice exhibit abnormal neuronal organization and seizures. Ann Neurol 52:285–296.

Verma P, Chierzi S, Codd AM, Campbell DS, Meyer RL, Holt CE, Fawcett JW (2005) Axonal protein synthesis and degradation are necessary for efficient growth cone regeneration. J Neurosci 25:331–342.

Way SW, McKenna J III, Mietzsch U, Reith RM, Wu HC, Gambello MJ (2009) Loss of *Tsc2* in radial glia models the brain pathology of tuberous sclerosis complex in the mouse. Hum Mol Genet 18:1252–1265.

Wenzel HJ, Cole TB, Born DE, Schwartzkroin PA, Palmitter RD (1997) Ultrastructural localization of zinc transporter-3 (ZnT-3) to synaptic vesicle membranes within mossy fiber boutons in the hippocampus of mouse and monkey. Proc Natl Acad Sci U S A 94:12676–12681.

Wenzel HJ, Born DE, Dubach MF, Gundersen VM, Maravilla KR, Robbins CA, Szot P, Zierath D, Schwartzkroin PA (2000a) Morphological plasticity in an infant monkey model of temporal lobe epilepsy. Epilepsia 41 [Suppl 6]:S70–S75.

Wenzel HJ, Woolley CS, Robbins CA, Schwartzkroin PA (2000b) Kainic acid-induced mossy fiber sprouting and synapse formation in the dentate gyrus of rats. Hippocampus 10:244–260.

West MJ, Slomianka L, Gundersen HJG (1991) Unbiased stereological estimation of the total number of neurons in the subdivisions of the rat hippocampus using the optical fractionator. Anat Rec 231:482–497.

Williams PA, Dou P, Dudek FE (2004) Epilepsy and synaptic reorganization in a perinatal rat model of hypoxia-ischemia. Epilepsia 45:1210–1218.

Williams PA, White AM, Clark S, Ferraro DJ, Swiercz W, Staley KJ, Dudek FE (2009) Development of spontaneous recurrent seizures after kainate-induced status epilepticus. J Neurosci 29:2103–2112.

Winokur RS, Kubal T, Liu D, Davis SF, Smith BN (2004) Recurrent excitation in the dentate gyrus of a murine model of temporal lobe epilepsy. Epilepsy Res 48:93–105.

Wuarin J-P, Dudek FE (1996) Electrographic seizures and new recurrent excitatory circuits in the dentate gyrus of hippocampal slices from kainate-treated epileptic rats. J Neurosci 16:4438–4448.

Wuarin J-P, Dudek FE (2001) Excitatory synaptic input to granule cells increases with time after kainate treatment. J Neurophysiol 85:1067–1077.

Zeng L-H, Xu L, Gutmann DH, Wong M (2008) Rapamycin prevents epilepsy in a mouse model of tuberous sclerosis complex. Ann Neurol 63:444–453.

Zeng L-H, Rensing NR, Wong M (2009) The mammalian target of rapamycin signaling pathway mediates epileptogenesis in a model of temporal lobe epilepsy. J Neurosci 29:6964–6972.

Zhan R-Z, Nadler JV (2009) Enhanced tonic GABA current in normotopic and hilar ectopic dentate granule cells after pilocarpine-induced status epilepticus. J Neurophysiol 102:670–681.

Zhang N, Houser CR (1999) Ultrastructural localization of dynorphin in the dentate gyrus in human temporal lobe epilepsy: a study of reorganized mossy fiber synapses. J Comp Neurol 405:472–490.

Zhang W, Yamawaki R, Wen X, Uhl J, Diaz J, Prince DA, Buckmaster PS (2009) Surviving hilar somatostatin interneurons enlarge, sprout axons, and form new synapses with granule cells in a mouse model of temporal lobe epilepsy. J Neurosci 29:14247–14256.

Zhang X, Cui S-S, Wallace AE, Hannesson DK, Schmued LC, Saucier DM, Honer WG, Corcoran ME (2002) Relations between brain pathology and temporal lobe epilepsy. J Neurosci 22:6052–6061.

Zhou J, Blundell J, Ogawa S, Kwon C-H, Zhang W, Sinton C, Powell CM, Parada LF (2009) Pharmacological inhibition of mTORC1 suppresses anatomical, cellular, and behavioral abnormalities in neural-specific *Pten* knockout mice. J Neurosci 29:1773–1783.